SEISMIC BEHAVIOR OF SLAB–COLUMN CONNECTIONS USING HIGH PERFORMANCE FIBER REINFORCED CONCRETES

António Ramos, Brisid Isufi, Rui Marreiros

Synopsis: Significant research efforts have been devoted to achieving high performance of slab – column connections subjected to lateral loading. Solutions such as using stirrups and headed studs have been shown to work well. With the development of concrete materials with enhanced properties, new possibilities have arisen to employ solutions that are easy to apply and cause less congestion of reinforcement. A total of nine tests on flat slab specimens subjected to combined gravity and lateral loading are discussed, including two new specimens with High Performance Fiber Reinforced Concrete (HPFRC) over a limited region near the column. The main experimental variables were the flexural reinforcement ratio and the punching shear improvement method: none, headed studs, High Strength Concrete (HSC) or HPFRC. It is shown that excellent behavior is achieved with a relatively small amount of HPFRC, extended up to 1.5 times the effective depth of the slab from the face of the column. Punching was completely avoided until the end of the loading protocol (6% drift) for the specimens with HPFRC, whereas reference specimens without punching shear reinforcement failed at 1% drift and specimens with HSC reached 3% drifts. Additionally, the use of HPFRC led to an increased unbalanced moment transfer capacity and lateral stiffness, though this effect was more pronounced for specimens with lower flexural reinforcement ratio.

Keywords: flat plate, flat slab, high performance fiber reinforced concrete, high strength concrete, punching shear, seismic loading.

INTRODUCTION

Flat slabs are often used to carry gravity loads in office and residential multi-story reinforced concrete buildings. When subjected to earthquakes, however, slab – column connections are more prone to fail in punching shear due to combined gravity and lateral loading. Throughout the years, different techniques have been developed to improve the deformation capacity of slab – column connections under lateral loading, i.e., to increase the drift capacity at which failure occurs. Traditional punching shear reinforcement systems such as stirrups and headed studs have been shown to be particularly efficient. However, the addition of stirrups or headed studs near the column, where a high density of longitudinal reinforcement is expected, can be a problem for the execution of works.

Various monotonic gravity loading tests conducted in the past indicate that advanced concrete materials such as HSC (Hallgren 1996; Inácio et al. 2015; Marzouk and A. Hussein 1991; Marzouk and Jiang 1997; Regan et al. 1993) or FRC (Gouveia, Faria, and Ramos 2019a; Harajli, Maalouf, and Khatib 1995; Landler and Fischer 2019; Swamy and Ali 1982) can be effective in increasing the punching shear strength of flat slabs. The promising results obtained for gravity loading conditions have motivated researchers to study the possibility of applying such materials also for seismic loading conditions.

A small number of specimens with HSC have been tested under reversed horizontal cyclic loading, by Emam et al (1997), Marzouk et al (2001) and more recently by Inácio et al. (2020). All these aforementioned tests have been conducted on 150 mm (5.91 in.) thick specimens. It is important to mention that only Inácio et al. (2020) used HSC with compressive strength above 100 MPa (14500 psi), which is possible nowadays due to the advancement of technology.

The number of lateral loading tests on specimens with FRC is larger than that of tests on HSC specimens, but the variations from one specimen to another are greater in case of FRC with regards to slab thickness, fiber volume fraction, test setup, flexural reinforcement ratios etc. (see Isufi and Pinho Ramos (2021)). Past tests include Durrani and Diaz (1992), Tegos and Tsonos (1996), Schreiber and Alexander (2001), Cheng and Parra-Montesinos (2010), Cheng et al (2010), Scotta and Giorgi (2016) and Gouveia et al (2019b).

Regardless of the differences, the aforementioned studies agree that HSC and FRC can significantly improve the performance of slab – column connections under seismic loading. Furthermore, several studies have shown that there is a great potential of economizing the use of these materials by applying them only in the vicinity of the column. For a more thorough literature review of past tests with HSC and FRC, the reader is referred to Isufi and Ramos (2021). The literature review of Isufi and Ramos (2021) showed that the combination of HSC with FRC has not been thoroughly explored as a solution for slab – column connections under seismic loading conditions.

In this paper, the possibility of using a High-Performance Fiber Reinforced Concrete (HPFRC) in the vicinity of the column to enhance the performance of slab – column connections under lateral loading is investigated. This material has a cylinder compressive strength of about 120 MPa (17400 psi), an improved behavior in tension and it is self-compacting. Having as a starting point, the good results obtained in previous tests of specimens using HSC near the column, the purpose of the new tests was to have a concrete with a similar compressive strength and the addition of fiber (HPFRC) and possibly optimize the region where the advanced concrete is added, with a reduction of costs. Two new specimens with HPFRC are presented in this paper. To study the behavior of these two new specimens, a total of nine specimens are analyzed, leading to the following experimental variables: 1) the flexural reinforcement ratio; 2) the punching shear improvement method: a) none, b) headed studs; c) HSC; d) HPFRC.

OVERVIEW OF HPFRC

The benefits of both HSC and FRC are manifested in a material often referred to as High Performance Fiber Reinforced Concrete (HPFRC). Although many variants of this material exist, the term “high performance” usually refers to other properties such as durability and workability in addition to the high strength.

A research project is currently under way at FCT NOVA, aiming to use a HPFRC recently developed by Blazy et al. (2021) and Nunes et al. (2021) at the central region of flat slab specimens subjected to monotonic vertical loading to failure and reversed horizontal cyclic loading with constant gravity loads. The HPFRC uses a Portland cement type CEM I 42.5R, limestone powder, silica fume and a high-range water reducer (superplasticizer). Fine and coarse aggregates with maximum aggregate size of 8 mm (0.32 in.) are also used. The total fiber volume fraction is 1%, but it should be mentioned that two types of fibers are used (Figure 1~~Figure 1~~) in equal proportions: 0.5% corresponding

to triple hooked-end long fibers (Dramix® 5D 65/60BG) and 0.5% corresponding to short straight fibers (Dramix® OL 13/.20).

(a) (b)

Figure 1 – Steel fibers used in the HPFRC: a) short straight fibers; b) triple hooked-end fibers

Table 1~~Table 1~~ summarizes the mix proportions of the HPFRC. To produce this concrete, a strict procedure is followed, starting with a careful weighing of its constituents. Subsequently, sand, coarse aggregates and a portion of the water are added to the mixer, mixed for 2.5 minutes followed by an absorption period of 5 minutes. In the next step, cement, limestone powder, silica fume, the remaining water and the superplasticizer are added and mixed for 5 minutes. Afterwards, fibers are added and mixed for 3 more minutes, after which the product is ready for casting (Blazy et al. 2021; Nunes et al. 2021).

Table 1 – Mix proportions of the HPFRC

Material	Quantity (kg/m^3)
Cement CEM I 42.5R	531.86
Limestone powder	203.72
Silica fume	53.19
Water	147.85
Superplasticizer	12.55
Fine aggregates	811.82
Coarse aggregates	721.43
Steel fibers (long)	39.25
Steel fibers (short)	39.25

Note: 1 kg/m^3 = 0.062 lb/ft^3

The resulting concrete is a self-compacting one, with a compressive strength of about 120 MPa (17400 psi) and a behavior in tension characterized by a limit of proportionality of 10 MPa (1450 psi), and f_{R1} to f_{R4} residual flexural strengths of 15.4, 18.0, 16.4 and 12.9 MPa (2233.0, 2610.0, 2378.0 and 1870.5 psi), respectively. These values were obtained through three-point bending tests, according to EN 14651:2005 + A1:2007 and the results of these tests are present in Figure 2~~Figure 2~~, where the nominal flexural stress versus crack mouth opening displacement relationship is presented for the 6 tests performed (Nunes et al. 2021).

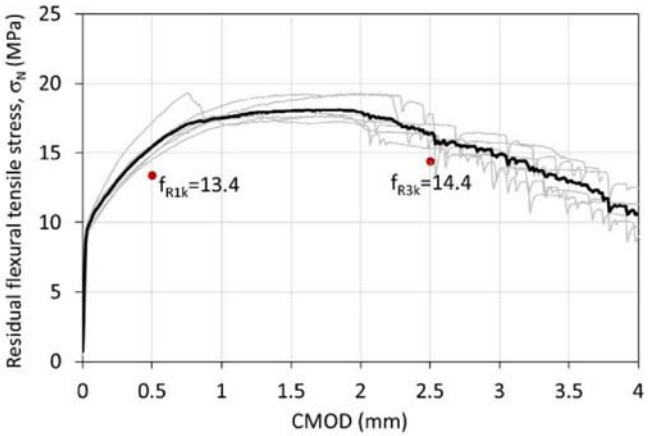

Figure 2 – σ_N vs CMOD curves for six tested specimens with the mean curve represented in black (extracted from Nunes et al. 2021) (Note: 1 MPa = 145 psi; 1 mm = 0.0394 in.)

DESCRIPTION OF THE EXPERIMENTS

Test setup

An experimental setup designed specifically to test flat slabs under combined gravity and lateral loading with continuity boundary conditions along the direction of lateral loading was designed and built at FCT NOVA. The specimens tested using this setup represent a section of the slab between mid-spans in the longitudinal direction and between lines of zero moment in the transversal direction. The first tests using this setup were published in Almeida et al. (2016) and they consisted of specimens without punching shear reinforcement, with a flexural reinforcement ratio of about 1% and different loading conditions (different gravity loads and different lateral loading protocols: monotonic and reversed cyclic). A schematic of the test setup as well as a detailed view are shown in Figure 3~~Figure 3~~.

The test setup has been described in detail in several publications in the past (Almeida et al. 2016; Ramos et al. 2017), but a brief description is provided herein. The test setup has three sub-systems, serving the following purposes:

- Sub-system "A" (see blue steel profiles in Figure 3~~Figure 3~~-b) consists of steel profiles forming a seesaw-like mechanism that ensures equal vertical displacement at the opposite edges of the specimen. These opposite edges correspond to two adjacent mid-span lines in a continuous flat slab, considering equal spans between columns and equal loads on all spans.
- Sub-system "B" (see green steel profiles in Figure 3~~Figure 3~~-b) consists of steel profiles cantilevered from the slab and an axially loaded strut that connects the two cantilever tips. The purpose of this sub-system is to enforce equal rotations at the opposite edges that correspond to mid-span lines.
- Sub-system "C" (see horizontal yellow steel profiles in Figure 3~~Figure 3~~-a) consists of spreader beams on top of the slab specimen, prestressing strands and beams under the slab that form a closed system that applies and maintains the gravity load and accompanies the slab during lateral loading.

Description of the specimens

Using the test setup described above, several tests were conducted throughout the last years. For the majority of these tests, the geometry, flexural reinforcement details and loading protocol were kept the same. The main variable between different experimental campaigns conducted throughout the years was the solution adopted to enhance the punching shear resistance, e.g., stirrups, studs, post-installed prestressed bolts. Stirrups were tested in Almeida et al. (2020), Isufi et al. (2019) tested headed studs, post-installed bolts were used as a strengthening method in Almeida et al. (2020), among other works. A summary of main conclusions from different experiments conducted using the test setup of Figure 3~~Figure 3~~ can be found elsewhere (Isufi et al. 2021).

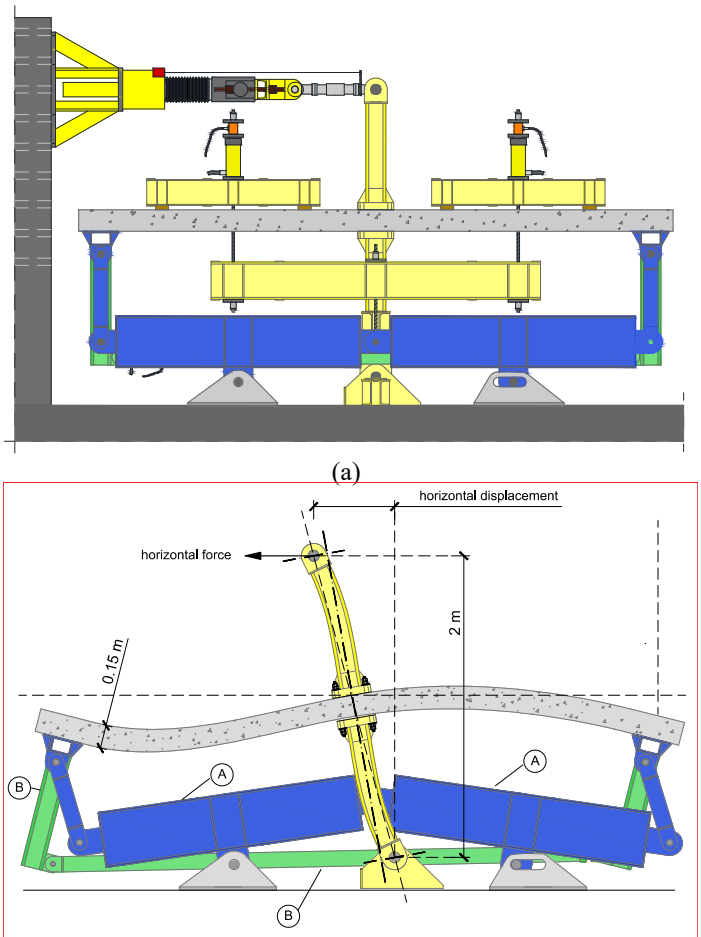

Figure 3 – Test setup developed at FCT NOVA: a) elevation of full test setup; b) sub-systems A and B under horizontal imposed displacements (not to scale) (Note: 1 m = 3.281 ft)

In this paper, a total of nine specimens, that are listed in Table 2~~Table 2~~, are analyzed, including two new specimens (not yet reported) with HPFRC. These new specimens are intended to be an evolution from the specimens with HSC already tested, reason why the HSC specimens are presented and compared. Results from specimens with normal concrete without punching shear reinforcement and specimens with shear studs will also be shown for comparison. The new specimens are designated as C-HP600-L and C-HP600-M, where "C" stands for "cyclic", "HP600" stands for "HPFRC square zone of size 600 mm (23.64 in.)" and "L" and "M" refer to the flexural reinforcement ratio: low (about 0.6%) and medium (about 1.0%). These designations were defined in a context where tests with three different amounts of reinforcement were conducted at FCT NOVA and from the lowest to the highest amount of reinforcement the slabs were classified as having low, medium or high ratios of reinforcement.

The names of the other specimens have not been changed from the original publications to prevent confusion of the readers. Two specimens with low flexural reinforcement ratio from Isufi et al. (2021) are included, one of them without any punching shear reinforcement (C-Ref-L) and the other reinforced with headed studs (C-SSR5-L). Two similar specimens but with higher flexural reinforcement ratio (considered "medium" for the purposes of this paper) are also included: C-50 from Almeida et al. (2016) without any punching shear reinforcement and C-SSR3 from Isufi et al. (2019) with headed studs.

The studs used in specimens C-SSR3 and C-SSR5-L were made of 8 mm (0.32 in.) deformed bars welded into steel plates forming a head of size at least 3 times the diameter of the stud for proper anchorage. The corresponding layouts are shown in Figure 4~~Figure 4~~, where the dimensions of the load bearing area (column) are also presented and are equal to 250 mm x 250 mm (9.84 in. x 9.84 in.). Although specimens with 5 rows of studs have been tested in Isufi et

al. (2019), C-SSR3 was chosen for its compressive concrete strength, that is comparable to that of the other specimens in Table 2~~Table 2~~.

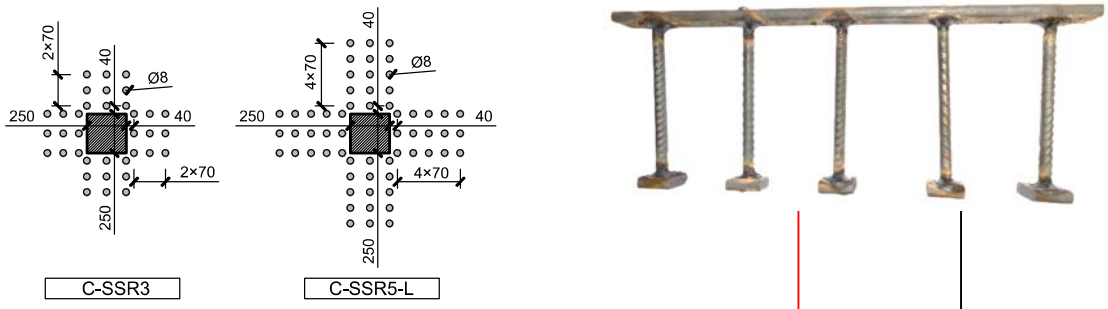

Figure 4 – Layout of studs in specimens C-SSR3 and C-SSR5-L and the side view of a set prepared for the 5 layers layout

Inácio et al. (2020) tested specimens with HSC, with a compressive strength of approximately 120 MPa (17400 psi). Three specimens were tested and reviewed in this paper, where the only significant difference between them was the geometry of the HSC zone. In one of the specimens (named CHSC1), HSC was applied in a layer at the bottom 50 mm (1.97 in.) of the slab, and it was extended over an area up to 1.9*d* from the face of the column (where *d* is the effective depth of the slab). Two other specimens with full-depth HSC extended up to 3.8*d* (CHSC2) and 2.5*d* (CHSC3) were also tested. The specimens are further described in Figure 5~~Figure 5~~, where the extent of the HSC or HPFRC zone is shown as a function of the effective depth (*d*). The concrete compressive cylinder strengths in vicinity of the column ($f_{c,HP}$) as well as the concrete compressive cylinder strengths in the rest of the slab (f_c) are shown for each specimen.

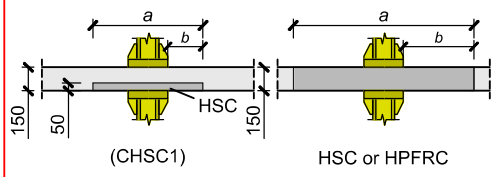

Specimen	Type	*a* (mm)	*b*	f_c (MPa)	$f_{c,HP}$ (MPa)
CHSC1	HSC	700	1.9*d*	61.6	115.2
CHSC2	HSC	1150	3.8*d*	45.9	120.2
CHSC3	HSC	850	2.5*d*	48.9	123.6
C-HP600-L	HPFRC	600	1.5*d*	52.6	116.8
C-HP600-M	HPFRC	600	1.5*d*	44.9	114.8

Figure 5 – Geometry of the HSC and HPFRC area in the specimens with these materials (Note: 1 mm = 0.0394 in.; 1 MPa = 145 psi)

Figure 5~~Figure 5~~ also includes the new specimens with HPFRC, namely C-HP600-L and C-HP600-M. An even lower extent of the zone with advanced concrete material was attempted in these specimens, only 1.5*d* from the face of the column. In both cases, the entire depth of the specimen was cast with the same material, unlike the case of CHSC1.

For the tested specimens with the so-called "low" reinforcement ratio (i.e., approximately 0.6%, see Table 2~~Table 2~~), the top flexural reinforcement consisted of 12 mm (0.47 in.) deformed bars with a spacing of 150 mm (5.91 in.) in the vicinity of the column and 200 mm (7.87 in.) beyond approximately 3*d* from the face of the column. For the tested specimens with the so-called "medium" reinforcement ratio (i.e., approximately 1.0%, see Table 2~~Table 2~~), the top flexural reinforcement consisted of 12 mm (0.47 in.) deformed bars with a spacing of 100 mm (3.94 in.) in the vicinity of the column and 200 mm (7.87 in.) beyond approximately 3*d* from the face of the column. Bottom reinforcement consisted of 10 mm (0.39 in.) deformed bars in both cases. Flexural reinforcement details are given in Figure 6~~Figure 6~~ for both flexural reinforcement layouts.

Table 2 – Summary of specimen's data and results

Specimen	Special feature	ρ (%)	f_c*	V_g (*kN*)	$F_{H,max}$ (*kN*)	$d_{r,FH,max}$ (%)	$d_{r,u}$ (%)
C-Ref-L (Isufi et al. 2021)	None	0.6	31.3	165	36.4	1.5	**1.0
C-SSR5-L (Isufi et al. 2021)	Headed studs	0.6	46.6	182	41.9	3.0	>6.0
C-HP600-L	HPFRC	0.6	52.6	182	56.4	4.0	>6.0
C-50 (Almeida et al. 2016)	None	1.0	52.4	203	37.4	1.0	1.0
C-SSR3 (Isufi et al. 2019)	Headed studs	1.0	41.2	196	60.4	3.5	4.0
C-HP600-M	HPFRC	1.0	44.9	200	70.5	4.0	>6.0
CHSC1 (Inácio et al. 2020)	HSC, partial	1.0	61.6	222	52.3	1.5	1.5
CHSC2 (Inácio et al. 2020)	HSC	1.0	45.9	200	55.8	2.5	3.0
CHSC3 (Inácio et al. 2020)	HSC	1.0	48.9	213	58.4	2.5	3.0

* concrete compressive strength corresponds to the conventional concrete. For compressive strength of HSC or HPFRC, refer to Figure 5~~Figure 5~~.
** specimen completed half a cycle at 1.5% drift, but the last completed cycle was at 1.0% drifts.
$F_{H,max}$, corresponds to maximum horizontal force.
$d_{r,FHmax}$, corresponds to the drift when $F_{H,max}$ is reached.
$d_{r,u}$, corresponds to the maximum drift attained before failure and is taken as the maximum drift attained before the horizontal load drops below 80% of $F_{H,max}$. For the specimens that did not fail before the end of the protocol, >6.0% appears in the table.

Note: 1 kN = 0.2248 kips

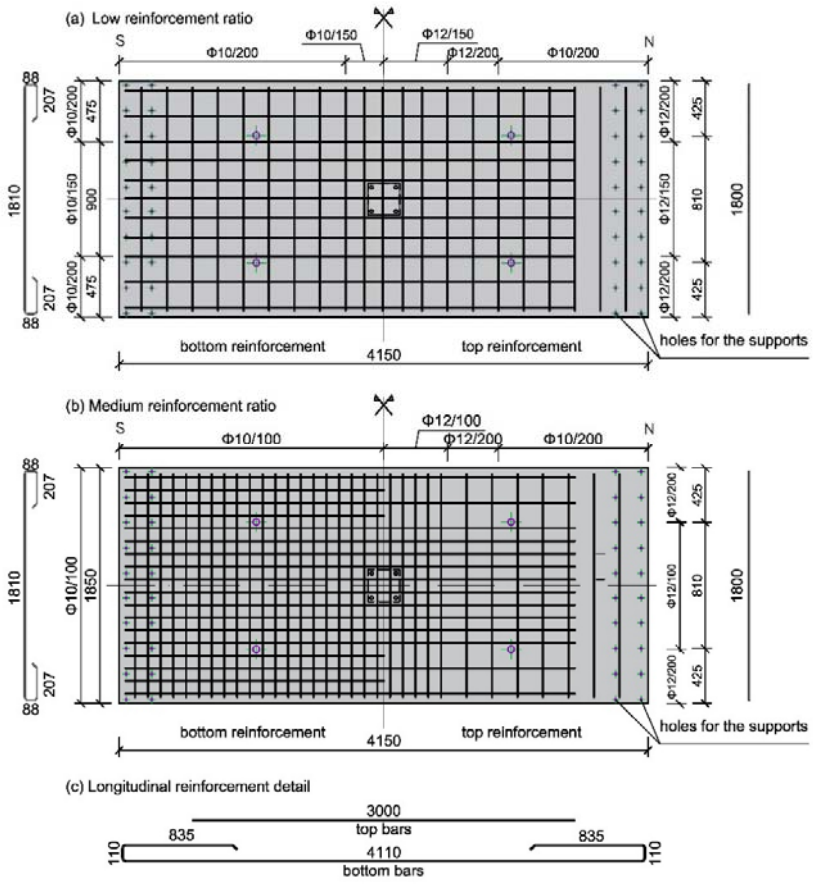

Figure 6 – Flexural reinforcement details: a) reinforcement ratio approximately 0.6%; b) reinforcement ratio approximately 1.0%; c) details (units in mm) (Note: 1 mm = 0.0394 in.)

Materials and loading protocol

Concrete compressive strengths measured on standard 150×300 mm (5.91x11.81 in.) cylinders are summarized in Table 2~~Table 2~~. To account for variations in concrete compressive strength, the ratio between the applied gravity load (V_g, see the values in Table 2~~Table 2~~ for each specimen) and the concentric punching shear strength (V_0), known as Gravity Shear Ratio (GSR), was kept approximately constant and around 50% for all specimens. The value of V_0 was calculated based on Eurocode 2, clause 6.4.4 (CEN 2004) with average material properties and no partial safety factors. To calculate V_0, the concrete strength f_c from Figure 5~~Figure 5~~ was used instead of $f_{c,HP}$. To calculate V_0, the critical perimeter at 2d from the face of the column was always used, once the principle was to have the slab with normal concrete as reference and then test different enhancement solutions, e.g., studs, HSC, HPFRC.

After the application of the target gravity load, V_g, this load was kept constant and reversed horizontal cyclic displacements were applied at the top of the column (see Figure 3~~Figure 3~~-b). Dividing the applied horizontal displacement by 2 m (6.562 ft) (see Figure 3~~Figure 3~~-b), the drift ratio is obtained. The loading protocol predicts target drifts starting from 0.5% to 6.0% with steps of 0.5% (Figure 7~~Figure 7~~). Drift cycles lower than 4.0% were repeated three times to study cyclic degradation due to repeated loading. Drifts at 4.0% were repeated twice, whereas larger drifts were imposed only once. The tests were stopped when a punching failure occurs, when the horizontal load drops significantly or when the end of the protocol was reached.

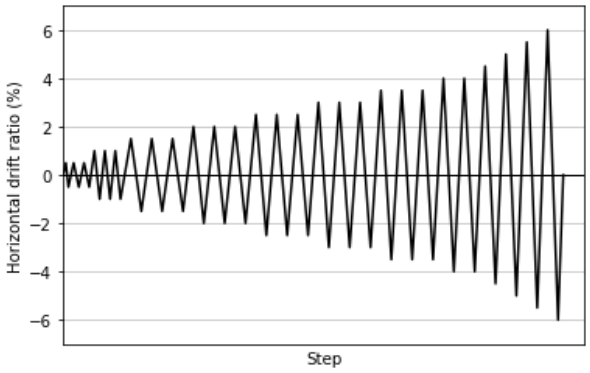

Figure 7 – Horizontal loading protocol

MAIN RESULTS

Cracking and failure modes

Three of the specimens presented in Table 2~~Table 2~~ reached the end of the loading protocol (at 6% drift) without suffering a punching shear failure. These specimens are C-SSR5-L and the two specimens with HPFRC: C-HP600-L and C-HP600-M. Although heavily cracked at 6% drift, these specimens were able to carry the gravity loads as well as sustain significant lateral loads (comparable to the maximum load, i.e. in an almost plastic plateau).

For all the non-shear-reinforced specimens that reached failure, this was marked by the development of a critical shear crack near the column, as it is typical for flat slabs without punching shear reinforcement. Failure was within the zone with advanced concrete material in all the specimens except CHSC1, where the shear crack crossed both layers, with HSC and normal concrete, since the HSC was only used on the bottom part of the slab in a thin layer, as explained before. In the specimens with headed studs, the punching shear failure occurred outside the shear-reinforced zone.

For detailed descriptions of the behavior of specimens, except the ones with HPFRC, the reader is referred to the original publications (Almeida et al. 2016; Inácio, Isufi, et al. 2020; Isufi et al. 2019; Isufi, Rossi, et al. 2021). For the specimens with HPFRC, the following section provides an overview of the behavior throughout the test.

Behavior of specimens with HPFRC

For both specimens (C-HP600-L and C-HP600-M), the application of gravity load was associated with the development of flexural cracks in the negative bending moment region of the slab specimen. Radial cracks of significant width were not detected during gravity loading. The application of horizontal drifts led to a continuous development of cracks in both specimens, although specimen C-HP600-L was notably more cracked and deflected (for the same drift ratio).

Positive bending moment cracks at the simulated mid-span (i.e., at the extremities of the specimen, running along the shorter direction) were detected in both specimens since the early stages of loading. As the specimens degraded due to cyclic lateral loading, these cracks grew wider and deeper. At around 3.0% drift ratios, positive bending moment cracks were detected also in the vicinity of the column, indicating bending moment sign reversal in the vicinity of the column due to significant unbalanced moments.

As previously mentioned, specimen C-HP600-L reached the end of the protocol (6% drift, after which the test cannot continue due to limitations of the setup) without suffering a brittle punching failure. At the end of the test (after a 6% drift cycle), the specimen was severely damaged in flexure, with cracks in the transverse direction (perpendicular to the application of horizontal load) being the dominating ones, and radial cracks being significantly narrower (see Figure 8~~Figure 8~~-a). Some signs of shear damage were also present, with a small intrusion of the steel column into the slab – column joint (Figure 8~~Figure 8~~-b) and peripheral cracks developing on the side of the column (on the top surface).

(a)

(b)

Figure 8 – Cracking of specimen C-HP600-L at the end of the test, at 6% drift: a) upper surface; b) bottom surface

Similarly, specimen C-HP600-M reached the end of the protocol without a punching shear failure. Significant cracking was present in the top surface at the end of the protocol (Figure 9~~Figure 9~~-a), although crack widths were smaller than in C-HP600-L. This is a normal and expected consequence of the higher flexural reinforcement ratio in C-HP600-M. Some crushing of the HPFRC in the vicinity of the column was present in the bottom face, and a small intrusion of the column into the slab – column joint region was also observed (Figure 9~~Figure 9~~-b).

In both specimens with HPFRC, cracks followed a natural pattern when crossing areas with different materials, i.e., cracks originating in the HPFRC zone continued throughout the zone with Normal Strength Concrete (NSC) and no significant discontinuities in the crack pattern were observed for the main flexural cracks. On the other hand, many cracks were developed and contained within the HPFRC zone, especially for high horizontal drift ratios. This behavior demonstrates both the compatibility of the two materials for structural applications and the ability of HPFRC to effectively control cracking.

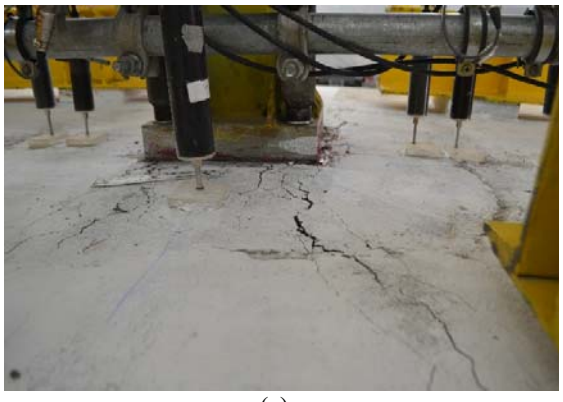

(a)

(b)

Figure 9 – Cracking of specimen C-HP600-M at the end of the test, at 6% drift: a) upper surface; b) bottom surface

Force – displacement relationship

For the specimens that reached failure, despite similar failure modes, the drift capacities were quite different. The highest drift was reached by the specimens that did not fail. These specimens reached the end of the protocol, corresponding to a maximum drift ratio of 6%. Specimens with HSC through the full depth (CHSC2 and CHSC3) also attained significant drift ratios (3.0%). The drift capacity was lower (equal to 1.5%) for the specimen with HSC applied only at the bottom 50 mm (1.97 in.) of the slab (CHSC1). Even though this is an improvement compared to reference specimens without HSC (for example, specimen C-50 in Almeida et al. (2016), with similar GSR and no punching shear reinforcement, made with a normal strength concrete, failed at 1% drift), the result shows that this solution of using a thin layer of HSC on the slab´s bottom surface might be inadequate for seismic loading, even if promising results had been obtained earlier for monotonic vertical loading (Inácio, Lapi, and Pinho Ramos 2020). The reason for this is that seismic loading changes the signs of the moments near the column, leading to the need to have the HSC material in the bottom and top of the slab to get improved results.

Figure 10~~Figure 10~~ shows horizontal load – displacement (drift ratio) curves for all the specimens. The behavior is fairly similar for all the specimens that reach high drift ratios, presenting stable hysteresis cycles with considerable pinching, and a low lateral stiffness as demonstrated by the high drifts at global slab – column connection yielding. Nonetheless, it is noticed that there are some differences in the horizontal force.

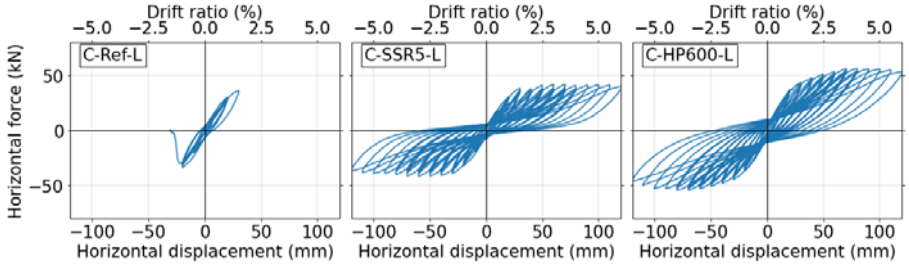

(a)

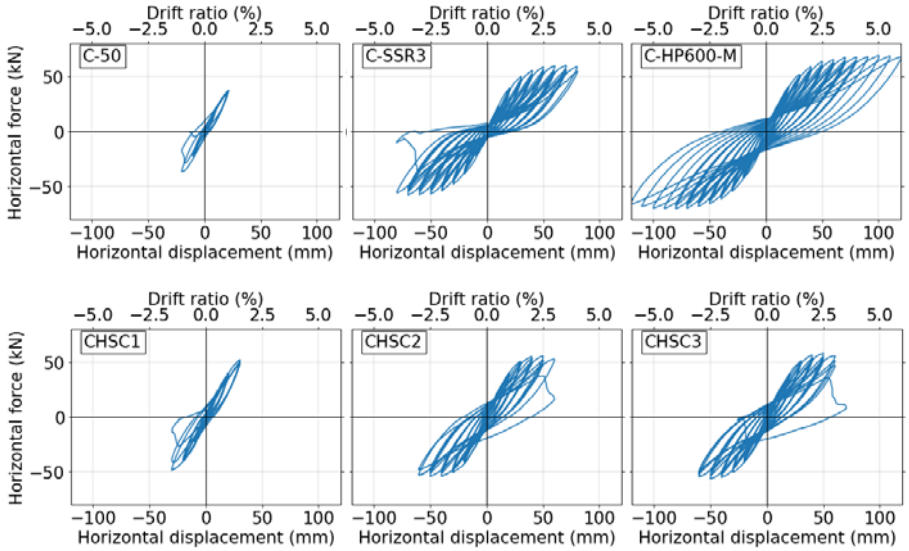

(b)

Figure 10 – Horizontal load – displacement (drift ratio) relationships: a) specimens with flexural reinforcement ratio approximately 0.6%; b) specimens with flexural reinforcement ratio approximately 1.0% (Note: 1 kN = 0.2248 kips; 1 mm = 0.0394 in.)

From **Figure 10**~~Figure 10~~, it is clear that the use of headed studs or the use of HPFRC are both viable solutions that can lead to a significant increase of the deformation capacity of slab – column connections. For both flexural reinforcement ratios (i.e., low and medium), the ultimate drift capacity was increased from only 1.0% in the specimens without punching shear reinforcement (C-Ref-L and C-50) to beyond 4.0%, which is a fairly high drift ratio for real buildings subjected to earthquakes. These improvements in the drift capacity result also in higher ductility levels. The displacement ductility can be defined as the ratio between the maximum displacement and the yielding displacement, and once not all the specimens reached failure and the reference specimens did not reach yielding it is not possible to quantify this parameter for all the slabs, but some considerations can be addressed. Comparing the reference specimens with the specimens with HPFRC and studs, it can be inferred that specimens that had presented a brittle failure changed to a ductile failure (see Figure 11~~Figure 11~~-a). Comparing the HPFRC with the HSC in Figure 11~~Figure 11~~-b, it can be concluded that the fibers were also fundamental for the ductility improvement.

When analyzing the horizontal loads, it is noticed that specimens with HPFRC, although over a small width of the specimen, reached higher horizontal loads compared to their counterparts with the same flexural reinforcement ratio but with headed studs. These observations are made clearer in Figure 11~~Figure 11~~-a, where the backbone curves for positive drifts are shown for specimens with HPFRC of different flexural reinforcement ratios as well as for the corresponding reference specimens (without punching shear reinforcement and with headed studs). It can be concluded that the fibers had a significant contribute for the bending moment resistance in the slab.

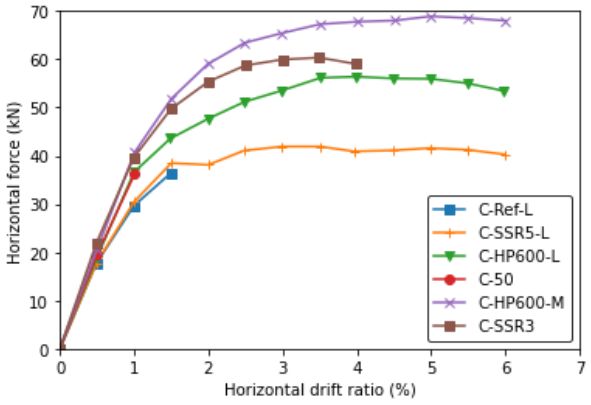

(a)

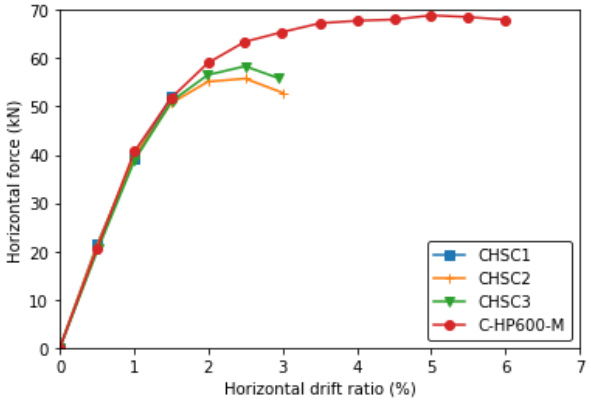

(b)

Figure 11 – Comparison of backbone curves: a) specimens with HPFRC compared to reference specimens with studs and without punching shear reinforcement; b) comparison between specimens with HSC and HPFRC (Note: 1 kN = 0.2248kips)

Evolution of secant stiffness

The secant stiffness is shown in Figure 12~~Figure 12~~ as a function of the slab – column connection rotation for the two specimens with HPFRC, their corresponding reference specimens with headed studs as well as one of the specimens with HSC (CHSC2). For simplicity and clarity, only one specimen with HSC is plotted, considering the similar behavior between CHSC2 and CHSC3 (refer to **Figure 10**~~Figure 10~~). The slab – column connection rotation is estimated by accounting for the elastic deformation of the steel column (see Figure 3~~Figure 3~~-b for a general idea of the deformed shape of the column). The deformation of the threaded rods was not considered, once the connection was designed to be a slip-resistant connection, with a large enough preloading of the rods to prevent separation of the steel base plate from the concrete. This leads to slab – column connections rotations slightly smaller than the target drifts. Also, for clarity, the results in Figure 12~~Figure 12~~ are shown only for the first excursion at each target drift ratio of the loading protocol. Finally, due to the rather symmetric behavior of the specimens (see **Figure 10**~~Figure 10~~), the calculation of the secant stiffness refers to positive drifts only.

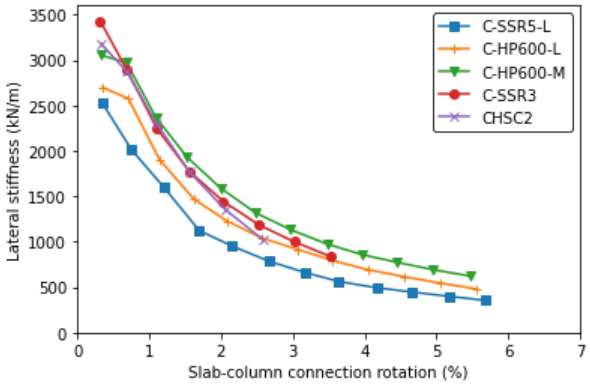

Figure 12 – Evolution of secant stiffness throughout the test (Note: 1 kN/m = 0.0685 kips/ft)

Several important observations can be made referring to Figure 12~~Figure 12~~. First, it is noticed that increasing the flexural reinforcement ratio leads to higher secant stiffnesses, as expected. Secondly, it is interesting to notice the role of HPFRC in the stiffness of the specimens. For the specimens with low flexural reinforcement ratio, HPFRC led to a significant increase of the secant stiffness throughout the entire test, whereas for the specimens with higher flexural reinforcement ratio (designated as "medium" in this paper) the effect of HPFRC was minimal at rotations up to around 1.0%, but an increased stiffness is observed in the specimen with HPFRC for higher drifts.

A comparison of the stiffness of HSC specimens with the others is only possible for medium reinforcement ratio based on the tests presented in this paper. Figure 12~~Figure 12~~ shows that this specimen is similar to the reference specimen with punching shear reinforcement in terms of stiffness (i.e., specimen C-SSR3), and the specimen with HPFRC (specimen C-HP600-M) has a higher secant stiffness for drifts above 1.0%. The reduction of secant stiffness in the HSC specimen (CHSC2) in the last cycle is due to failure of this specimen in punching shear.

PRACTICAL ASPECTS RELATED TO EXECUTION OF WORKS

Several lessons relevant for the execution of works were learned while preparing various specimens presented in this paper, with HSC and HPFRC. Although these materials behave differently during casting, all specimens have in common the necessity of separating wet conventional concrete from these advanced concrete materials and the requirement for monolithic behavior after curing. In the case of HSC, it was found that the most suitable solution is to cast the zone with advanced concrete material first, then cast the rest of the slab soon after (see Figure 13~~Figure 13~~-a). Due to the self-compacting property of the HPFRC used, the contrary was done: HPFRC was cast last (see Figure 13~~Figure 13~~-b). To contain the concrete from moving from one zone to the other, a general-purpose galvanized steel mesh with diameter 0.5 mm (0.02 in.) and 13 mm (0.51 in.) spacing was used in all cases, although more specialized products exist in the market.

Satisfactory results were obtained using the aforementioned casting procedures. The results and observations in general show that the final product worked as intended, with a monolithic behavior of the flat slab.

The different shrinkage properties of different concretes were a cause of concern. To mitigate this issue, the specimens were covered by a blanket that was kept humid all the time, covered by a plastic sheet to avoid excessive water evaporation during the first few days after casting. In the case of HPFRC, some cracking occurred on the top surface, regardless. Cracking occurred mainly at the interface between HPFRC and conventional concrete. For specimens that were previously tested under vertical monotonic loading to failure (not reported here), a closer inspection revealed that these shrinkage cracks were only superficial, going up to roughly 20 mm (0.79 in.) in depth. Furthermore, these cracks seemed to have no effect on the failure mode of the specimens. It should be noted that these shrinkage cracks were on the top face of the slab, where cracking due to negative bending moments near the column is expected to occur. Nonetheless, special attention and further research is needed during execution of works in cases where HPFRC is used for the purpose of improving the serviceability of slab – column connections. For seismic loading, the issue is generally not concerning.

For large-scale applications, it is recommended to perform casting of different concretes at approximately the same time whenever possible.

(a)

(b)

Figure 13 – Casting sequence: a) HSC and FRC specimens; b) HPFRC specimens

CONCLUSIONS

A series of tests conducted at FCT NOVA were described in this paper. The main purpose was to study the applicability of HPFRC over a small region near the column to improve the seismic behavior of slab – column connections while economizing the use of materials. Two new specimens are presented and compared to previously published specimens using the same test setup and loading conditions.

It was shown that an excellent behavior can be achieved by using HPFRC near the column and NSC over the rest of the slab. Compared to reference specimens that failed in punching at only 1.0% drift ratio, the two specimens with HPFRC reached 6.0% drift ratios without failing in punching.

The behavior of the specimens with HPFRC was significantly improved even compared to specimens with HSC that failed at 3.0% drift. The specimens with HPFRC had a comparable compressive strength with that of the specimens with HSC, and the improved behavior can be attributed to the addition of steel fibers.

The results presented in this paper show that there is a great potential of economizing the use of HPFRC. Punching shear failure was prevented until the end of the protocol (6% drift) with an area with HPFRC extended only up to 1.5 times the effective depth of the slab from the face of the column, for both flexural reinforcement ratios considered in this paper. In contrast, the specimens with HSC failed at 3.0% drift with an extent of the HSC zone at least 2.5 times the effective depth. This promising result needs to be checked for thicker slabs in the future.

When comparing the solutions with HPFRC with the solutions with studs that were tested, it can be concluded that both can reach similar drifts. The HPFRC resulted in higher values of horizontal forces than the solutions with studs due to the added flexural capacity given by the use of fibers.

Besides the increase of the ultimate drift capacity, it was shown that the application of HPFRC leads to an increase of the secant stiffness and the unbalanced moment transfer capacity of the slab – column connection. It was shown that this effect is more pronounced in slab – column connections with lower flexural reinforcement ratio.

ACKNOWLEDGEMENTS

The authors are grateful to Fundação para a Ciência e Tecnologia (FCT) - Ministério da Ciência, Tecnologia e Ensino Superior for the support through Project PTDC/ECI-EST/30511/2017. This work is also part of the research activity carried out at Civil Engineering Research and Innovation for Sustainability (CERIS) and with further funding by Fundação para a Ciência e a Tecnologia (FCT) in the framework of project UIDB/04625/2020

REFERENCES

Almeida, André F. O., Bruno Alcobia, Miguel Ornelas, Rui Marreiros, and António Pinho Ramos. 2020. “Behaviour of Reinforced-Concrete Flat Slabs with Stirrups under Reversed Horizontal Cyclic Loading.” *Magazine of Concrete Research* 72(7):339–56.

Almeida, André F. O., Micael M. G. Inácio, Válter J. G. Lúcio, and António Pinho Ramos. 2016. “Punching Behaviour of RC Flat Slabs under Reversed Horizontal Cyclic Loading.” *Engineering Structures* 117:204–19.

Almeida, André F. O., António Pinho Ramos, Válter Lúcio, and Rui Marreiros. 2020. “Behavior of RC Flat Slabs with Shear Bolts under Reversed Horizontal Cyclic Loading.” *Structural Concrete* 21(2):501–16.

Blazy, Julia, Sandra Nunes, Carlos Sousa, and Mário Pimentel. 2021. “Development of an HPFRC for Use in Flat Slabs.” *RILEM Bookseries* 30:209–20.

CEN. 2004. *EN 1992-1-1. Eurocode 2 — Design of Concrete Structures. Part 1-1: General Rules and Rules for Buildings*.

Cheng, Min-Yuan, Gustavo J. Parra-Montesinos, and Carol K. Shield. 2010. “Shear Strength and Drift Capacity of Fiber-Reinforced Concrete Slab-Column Connections Subjected to Biaxial Displacements.” *Journal of Structural Engineering* 136(9):1078–88.

Cheng, My and Gj Parra-Montesinos. 2010. “Evaluation of Steel Fiber Reinforcement for Punching Shear Resistance in Slab-Column Connections - Part II: Lateral Displacement Reversals.” *ACI Structural Journal* 107(01):110–18.

Durrani, A. J. and A. J. Diaz. 1992. “Seismic Resistance of Fiber-Reinforced Slab-Column Connections.” Pp. 3113–16 in *Earthquake Engineering, Tenth World Conference*. Rotterdam: Balkema.

Emam, Mohamed, H. Marzouk, and M. Sameh Hilal. 1997. “Seismic Response of Slab-Column Connections Constructed with High-Strength Concrete.” *ACI Structural Journal* 94(2):197–205.

EN 14651:2005+A1:2007(E) Test method for metallic fibre concrete – measuring the flexural tensile strength (limit of proportionality (LOP), residual). *CEN European Committee for Standardization*.

Gouveia, Nuno D., Duarte M. V. Faria, and António Pinho Ramos. 2019a. “Assessment of SFRC Flat Slab Punching Behaviour – Part I: Monotonic Vertical Loading.” *Magazine of Concrete Research* 71(11):587–98.

Gouveia, Nuno D., Duarte M. V. Faria, and António Pinho Ramos. 2019b. “Assessment of SFRC Flat Slab Punching Behaviour – Part II: Reversed Horizontal Cyclic Loading.” *Magazine of Concrete Research* 71(1):26–42.

Hallgren, Mikael. 1996. “Punching Shear Capacity of Reinforced High Strength Concrete Slabs.” KTH Royal Institute of Technology.

Harajli, M. H., D. Maalouf, and H. Khatib. 1995. “Effect of Fibers on the Punching Shear Strength of Slab-Column Connections.” *Cement and Concrete Composites* 17(2):161–70.

Inácio, Micael, Brisid Isufi, Massimo Lapi, and António Pinho Ramos. 2020. “Rational Use of High-Strength Concrete in Flat Slab-Column Connections under Seismic Loading.” *ACI Structural Journal* 117(6):297–310.

Inácio, Micael, Massimo Lapi, and Antonio Pinho Ramos. 2020. “Punching of Reinforced Concrete Flat Slabs – Rational Use of High Strength Concrete.” *Engineering Structures* 206:110194.

Inácio, Micael M. G., André F. O. Almeida, Duarte M. V. Faria, Válter J. G. Lúcio, and António Pinho Ramos. 2015. “Punching of High Strength Concrete Flat Slabs without Shear Reinforcement.” *Engineering Structures* 103:275–84.

Isufi, Brisid, André Almeida, Rui Marreiros, António Pinho Ramos, and Válter Lúcio. 2021. “Slab – Column Connection Punching and Ductility Improvement Methods for Seismic Response of Buildings with Flat Slabs.” *(Submitted for Publication)*.

Isufi, Brisid and António Pinho Ramos. 2021. “A Review of Tests on Slab-Column Connections with Advanced Concrete Materials.” *Structures* 32(May 2020):849–60.

Isufi, Brisid, António Pinho Ramos, and Válter Lúcio. 2019. “Reversed Horizontal Cyclic Loading Tests of Flat Slab Specimens with Studs as Shear Reinforcement.” *Structural Concrete* 20(1):330–47.

Isufi, Brisid, Mariana Rossi, and António Pinho Ramos. 2021. “Influence of Flexural Reinforcement on the Seismic Performance of Flat Slab – Column Connections.” *Engineering Structures* 242(September):112583.

Landler, Josef and Oliver Fischer. 2019. “Steigerung Der Durchstanztragfähigkeit Und Duktilität Durch Die Zugabe Moderner Hochleistungsstahlfasern.” *Beton- Und Stahlbetonbau*.

Marzouk, H. and A. Hussein. 1991. “Experimental Investigation on the Behavior of High-Strength Concrete Slabs.” *ACI Structural Journal* 88(6):701–13.

Marzouk, H. and Dajiu Jiang. 1997. “Experimental Investigation on Shear Enhancement Types for High-Strength Concrete Plates.” *ACI Structural Journal* 94(1):49–58.

Marzouk, H., Moustafa Osman, and A. Hussein. 2001. “Cyclic Loading of High-Strength Lightweight Concrete Slabs.” *ACI Structural Journal* 98(2):207–14.

Nunes, Sandra, Mário Pimentel, and Carlos Sousa. 2021. “Mechanical and Fracture Behaviour of an Hpfrc.” in *BEfib2021*. Valencia: RILEM-fib.

Ramos, António, Rui Marreiros, André Almeida, Brisid Isufi, and Micael Inácio. 2017. “Punching of Flat Slabs under Reversed Horizontal Cyclic Loading.” Pp. 253–72 in *ACI Special Publication*. Vol. 315, edited by C. E. Ospina, D. Mitchell, and A. Muttoni. ACI, fib.

Regan, P. E., A. Al-Hussaini, K. E. Ramdane, and H. Y. Xue. 1993. “Behaviour of High Strength Concrete Slabs.” Pp. 761–73 in *Concrete 2000*, edited by R. K. Dhir and M. R. Jones. E & FN Spon.

Schreiber, Sascha K. and Scott D. B. Alexander. 2001. *Punching Shear Capacity of Slab-Column Connections with Steel-Fibre Reinforcement under Lateral Cyclic Loading*. Edmonton, Alberta, Canada.

Scotta, Roberto and Paolo Giorgi. 2016. “Comparative Cyclic Tests of Exterior Flat Slab–Column Connections in Normal Concrete and Fiber-Reinforced Lightweight Aggregate Concrete.” *Materials and Structures* 49(10):4049–67.

Swamy, R. N. and S. A. R. Ali. 1982. “Punching Shear Behavior of Reinforced Slab-Column Connections Made with Steel Fiber Concrete.” *ACI Journal Proceedings* 79(5).

Tegos, J. A. and A. G. Tsonos. 1996. “Punching Strength Decay of Slab-Column Connections under Seismic Loading.” P. Paper No. 654 in *Eleventh World Conference on Earthquake Engineering 11WCEE*. Acapulco, Mexico: Elsevier Science Ltd.

Brief authors bio:

António Ramos is an Associate Professor with Habilitation at NOVA School of Science and Technology, Portugal. He received his Ph.D. degree in Civil Engineering / Structures (2003) from Instituto Superior Técnico, University of Lisbon and also holds a M.Sc. degree in Structural Engineering and a B.Eng in Civil Engineering from University of Lisbon. His research interests include flat slab structures, repair and strengthening of concrete structures and seismic behavior of structures.

Brisid Isufi is a postdoctoral researcher at NOVA School of Science and Technology, Portugal. He received his Ph.D. from the same institution in 2018, and B.Eng. and M.Sc. degrees from Polytechnic University of Tirana, Albania, in 2009 and 2011 respectively. His research interests include seismic behavior of slab–column connections, punching shear in flat slabs and earthquake engineering.

Rui Marreiros is an Assistant Professor at NOVA School of Science and Technology, Portugal. His research interests are: behavior of flat slab structures, seismic behavior of structures and seismic design of self-centering precast/prestressed buildings rocking.